

Impact of the Non-Gaussian Measurement Noise on the Performance of State-of-the-Art State Estimators for Distribution Systems

Stefan Čubonović¹, Dragan Četenović¹, Aleksandar Ranković¹

Abstract: This paper aims to investigate the impact of non-Gaussian measurement noise on state estimation (SE) results in distribution systems. To this end, the measurement noise is assumed to be distributed according to Gaussian or one of the following non-Gaussian probability distribution functions: Uniform, Laplace, Weibull and Gaussian mixture of two Gaussian components. The influence is investigated on three different state-of-the-art SE methods: weighted least squares (WLS) based static SE method, and two Kalman filter based forecasting-aided SE methods, namely extended Kalman filter (EKF) and unscented Kalman filter (UKF). Analyses are conducted on modified IEEE 37-bus system under different operating conditions, including quasi-steady state, sudden state changes and bad data. Performance of the methods in the presence of non-Gaussian measurement noise is compared against their performance when measurement noise is Gaussian distributed. The main conclusions were drawn, summarizing the impacts non-Gaussian measurement noise has on SE and proposing the solutions for overcoming some of the negative impacts.

Keywords: Distribution systems, Extended Kalman filter, Non-Gaussian measurement noise, State estimation, Unscented Kalman filter, Weighted least square.

1 Introduction

The task of SE is to provide accurate estimates of bus voltage phasors under wide range of operating conditions, including quasi-steady state operation, sudden state changes and bad data. Although SE of transmission systems has reached a certain level of maturity, SE of distribution systems still faces many difficulties. It is very important to overcome these difficulties because results of distribution system SE are being used for network reconfiguration, voltage/var control, distributed generation (DG) control, demand-side integration, contingency analysis, capacitor switching etc.; therefore, inaccurate state estimates can lead to wrong control decisions. One of the difficulties that threatens the accuracy of distribution system SE is intensified integration of

¹University of Kragujevac, Faculty of Technical Sciences Čačak, Serbia;

E-mails: stefan.cubonovic@ftn.kg.ac.rs; dragan.cetenovic@ftn.kg.ac.rs; aleksandar.rankovic@ftn.kg.ac.rs

intermittent DGs because it introduces more uncertainties into estimation results. Presence of bad data is an old ailment of distribution system SE that has persisted to this day since the lack of telemetry still remains at the distribution level. Lack of telemetry can also lead to loss of observability of the distribution system, making the SE feasible only in observable islands. Finally, the measurement noise statistics are usually not well known, so they are subject to certain assumptions. This paper investigates how statistics of measurement noise, especially if they are wrongly assumed, can affect the SE.

The most common assumption in state estimation (SE) is that measurement errors are independent, identically distributed and follow Gaussian distribution with zero mean. In practice, telemetered measurements collected using different metering devices (smart meters or different types of synchronized measurement devices (SMDs) including phasor measurement units (PMUs), microPMU, SMD-R etc. [1]), do not necessarily contain a noise that follows a Gaussian distribution [2]. This can be due to the electromagnetic interference in communication channels, and due to other sources of communication noise that can originate from natural causes (such as bad weather conditions) or artificial causes (such as technology based on inverters) [3, 4]. Obviously, there is a possibility of occurrence of non-Gaussian measurement noise in SE. If the same occurs, the performance of state estimators should be reconsidered.

In distribution systems, there is a limited number of installed conventional metering devices. In addition, SMDs are still not widely implemented in the distribution systems. To improve the measurement redundancy, unavailable measurements are commonly replaced with pseudo and/or virtual measurements. Pseudo measurements represent power injections of unmonitored loads obtained from the normalized daily load profiles, or power injections of the DGs calculated from the external inputs (wind speed, solar irradiance, water inflow predictions, etc.). As such, pseudo measurements are less accurate than telemetered measurements; they can contain measurement errors up to 50% and decrease the accuracy of SE, especially in case of poorly monitored distribution systems [5 – 7]. The errors contained in pseudo measurements do not necessarily follow a Gaussian distribution either. Conversely, virtual measurements represent zero active and reactive power injections into the buses without connected demand or DGs. Since these injections are known exactly, virtual measurements are highly accurate. As such, virtual measurements improve the accuracy of SE.

To handle non-Gaussian noise in pseudo measurements, Bayesian estimator is proposed [8]. Also, Bayesian estimator in [9] utilizes forecasted information and measurements on power flows, which can express non-Gaussian behavior. Transformed likelihood estimation method [10] and two robust state estimation methods founded on the conventional cubature particle filter [11] were used for state estimation and bad data detection in distribution networks to deal with the

non-Gaussian distributed measurement noise. Analysis of bad data, utilizing the largest normalized residual test, is used to detect, identify, and correct/eliminate multiple measurements with gross errors under both Gaussian and non-Gaussian noises [12]. In [13], authors investigated how a non-Gaussian measurement noise affects the distribution of the state vector of a linear Kalman filter. Cumulants (mean and variance) are used as a criterion to define the deviation of a non-Gaussian distribution from the Gaussian. However, a work that thoroughly investigates impacts of different types of non-Gaussian measurement noise on the performance of most frequently used state estimators under variety of operating conditions, summarizes them in one place and provides general conclusions, is still missing.

To address the above, in this paper, the performance of a static SE and two forecasting-aided SE are tested under the assumption that the telemetered and pseudo measurements are with non-Gaussian type of measurement noise. The different types of non-Gaussian probability density functions are assigned to the measurement noise, namely Uniform, Laplace, Weibull and Gaussian mixture. Then, the performance of the state estimators is compared against their performance in the presence of Gaussian distributed measurement noise. The comparison is made under different operating conditions, including quasi-steady state operation and sudden state changes. To make the comparison complete, performance is also compared from the perspective of bad data detection.

The remaining sections of the paper are structured as follows. The Section II presents three different estimation algorithms: WLS based static SE method and two Kalman filter based forecasting-aided SE methods (EKF and UKF). In the Section III, different types of non-Gaussian probability density functions are introduced. In Section IV, simulations and comparative analysis are conducted on modified IEEE 37-bus system. Finally, the primary conclusions are formulated in Section V.

2 State Estimation Methods

The state transition function describes how the system's state evolves over the time. Mathematically, the state transition function can be expressed as [14]:

$$\mathbf{x}^{(j+1)} = \mathbf{F}^{(j)} \mathbf{x}^{(j)} + \mathbf{g}^{(j)} + \mathbf{w}^{(j)}, \quad (1)$$

where:

$\mathbf{x} = [\mathbf{V}^T, \theta^T]^T$ – $n \times 1$ dimensional vector of the state variables, i.e., bus voltage magnitudes \mathbf{V} and phase angles θ ;

\mathbf{F} – $n \times n$ dimensional state transition matrix;

\mathbf{g} – $n \times 1$ dimensional vector associated with the trend behavior of the state trajectory;

\mathbf{w} – $n \times 1$ process noise vector accounting for uncertainties in the state transition function;

j – time instant; and

n – total number of state variables.

The association between measurements and state variables is called the measurement function and is mathematically expressed as [15]:

$$\mathbf{z}^{(j)} = \begin{bmatrix} z_1^{(j)} \\ z_2^{(j)} \\ \vdots \\ z_m^{(j)} \end{bmatrix} = \begin{bmatrix} h_1(x_1^{(j)}, x_2^{(j)}, \dots, x_n^{(j)}) \\ h_1(x_1^{(j)}, x_2^{(j)}, \dots, x_n^{(j)}) \\ \vdots \\ h_m(x_1^{(j)}, x_2^{(j)}, \dots, x_n^{(j)}) \end{bmatrix} + \begin{bmatrix} e_1^{(j)} \\ e_2^{(j)} \\ \vdots \\ e_m^{(j)} \end{bmatrix} = \mathbf{h}(\mathbf{x}^{(j)}) + \mathbf{e}^{(j)}, \quad (2)$$

where:

\mathbf{z} – $m \times 1$ measurement vector including telemetered, pseudo and virtual measurements;

\mathbf{h} – $m \times 1$ nonlinear vector-valued function;

\mathbf{e} – $m \times 1$ vector of measurement noise; and

m – total number of measurements.

To ensure observability of the entire system, the following condition must be satisfied: $m \geq n$. In addition, the minimum necessary measurement redundancy must be achieved at all buses in the system.

2.1 WLS objective function

Static SE relies only on the measurements collected at the current time instant and, therefore, utilizes the measurement model (2) only. Static SE can be treated as a typical WLS problem, where the objective function is the sum of the weighted squares of measurement residuals [16]:

$$J(\mathbf{x}) = [\mathbf{z} - \mathbf{h}(\mathbf{x})]^T \mathbf{R}^{-1} [\mathbf{z} - \mathbf{h}(\mathbf{x})], \quad \mathbf{R} = \text{diag} \{ \sigma_1^2, \sigma_2^2, \dots, \sigma_m^2 \}, \quad (3)$$

where \mathbf{R} is a diagonal covariance matrix whose diagonal elements are the variances of measurement noise. If measurement noise is Gaussian distributed, standard deviation σ_i of i^{th} telemetered or pseudo measurement can be calculated from the measurement accuracy (Acc) as [17]:

$$\sigma_i = \text{Mean}_i \left(\frac{Acc_i}{300} \right), \quad i = 1, 2, \dots, m. \quad (4)$$

The goal of optimization is to find state vector \mathbf{x} that will minimize the objective function (3), i.e., $\min_{\mathbf{x}} \{ J(\mathbf{x}) \}$ [15, 18 – 20]. To simplify the notation in (3), the superscript denoting the time instant has been omitted.

2.2 WLS SE method

The method most frequently used to minimize the objective function is by applying the Newton-Raphson method [18]. Using Newton-Raphson iterative method, the increment of state vector is calculated in each iteration k as:

$$\Delta \mathbf{x}^{(k+1)} = \mathbf{G}(\mathbf{x}^{(k)})^{-1} \mathbf{H}^{(k)}(\mathbf{x}^{(k)})^T \mathbf{R}^{-1} \Delta \mathbf{z}^{(k)}, \quad (5)$$

where:

$$\mathbf{G}(\mathbf{x}^{(k)}) = \mathbf{H}^{(k)}(\mathbf{x})^T \mathbf{R}^{-1} \mathbf{H}^{(k)}(\mathbf{x}) - \text{Information matrix};$$

$$\mathbf{H}(\mathbf{x}^{(k)}) = \frac{\partial \mathbf{h}(\mathbf{x})}{\partial \mathbf{x}} - \text{Jacobian matrix.}$$

2.3 KF objective function

In forecasting aided SE, state transition function (1) is utilized in addition to the measurement function (2). System of equations (1) and (2) can be solved in the Kalman filter framework. In this case, the objective function is extended by an additional term representing the sum of the weighted squares of differences between system states and their predictions [21]:

$$J(\mathbf{x}) = [\mathbf{z} - \mathbf{h}(\mathbf{x})]^T \mathbf{R}^{-1} [\mathbf{z} - \mathbf{h}(\mathbf{x})] + [\mathbf{x} - \mathbf{x}_-]^T \mathbf{P}_-^{-1} [\mathbf{x} - \mathbf{x}_-], \quad (6)$$

where:

\mathbf{x}_- – $n \times 1$ dimensional vector of state predictions;

\mathbf{P}_- – $n \times n$ dimensional state prediction error covariance matrix.

The solution is being obtained by minimizing the objective function (6). If system of equations (1) and (2) is linear, the solution can be obtained by applying classical Kalman filter. If this is not the case, different approximations are available to deal with the system nonlinearities.

2.4 EKF and UKF based SE methods

The EKF is based on the approximation of nonlinear function by the Taylor polynomial. First order EKF implies calculation of the first partial derivatives of the nonlinear function with respect to state variables in the vicinity of the linearization point, aiming to obtain a Jacobian matrix. The UKF uses the unscented transformation instead of linearization, avoiding the calculation of Jacobian matrix. With this variant of Kalman filter, limitations of EKF are exceeded [22], especially for highly nonlinear systems. Regardless of the variant used, Kalman filter based SE has three fundamental steps: parameter identification, state prediction and state estimation. These steps are described via equations and summarized in **Table 1** [14, 23, 24].

Table 1
Summary of equations for Kalman filter based state estimation methods.

EKF	UKF
Parameter identification	
$\alpha, \beta, \mathbf{Q}, \mathbf{R}, \mathbf{a}, \mathbf{b}$.	$\alpha_{\text{UKF}}, \beta_{\text{UKF}}, \kappa_{\text{UKF}}, \mathbf{Y}$ $w_m^{(0)}, w_c^{(0)}, w_m^{(i)}, w_c^{(i)}, \lambda_{\text{UKF}} \quad i = 1, 2, \dots, 2n.$
State prediction	
Assuming that \mathbf{x}_+ and \mathbf{P}_+ at time step j are known, the system state at time step $j+1$ can be forecasted in the following way: $\mathbf{x}_-^{(j+1)} = \mathbf{F}^{(j)} \mathbf{x}_+^{(j)} + \mathbf{g}^{(j)};$ $\mathbf{P}_-^{(j+1)} = \mathbf{F}^{(j)} \mathbf{P}_+^{(j)} (\mathbf{F}^{(j)})^T + \mathbf{Q}^{(j)}.$	$\mathbf{Y}_+^{(j)} = \mathbf{x}_+^{(j)} \mathbf{1}^T + \sqrt{n + \lambda} \begin{bmatrix} 0 & \sqrt{\mathbf{P}_+^{(j)}} & -\sqrt{\mathbf{P}_+^{(j)}} \end{bmatrix};$ $\hat{\mathbf{X}}^{(j+1)} = \mathbf{F}^{(j)} \mathbf{Y}_+^{(j)} + \mathbf{g}^{(j)} \mathbf{1}^T;$ $\mathbf{x}_-^{(j+1)} = \hat{\mathbf{X}}^{(j+1)} \mathbf{w}_m;$ $\mathbf{P}_-^{(j+1)} = \hat{\mathbf{X}}^{(j+1)} \mathbf{W} (\hat{\mathbf{X}}^{(j+1)})^T + \mathbf{Q}^{(j)}.$
State estimation	
$\mathbf{v}^{(j+1)} = \mathbf{z}^{(j+1)} - h(\mathbf{x}_-^{(j+1)});$ $\mathbf{S}^{(j+1)} = \mathbf{H}^{(j+1)} \mathbf{P}_-^{(j+1)} (\mathbf{H}^{(j+1)})^T + \mathbf{R}^{(j+1)};$ $\mathbf{K}^{(j+1)} = \mathbf{P}_-^{(j+1)} (\mathbf{H}^{(j+1)})^T (\mathbf{S}^{(j+1)})^{-1};$ $\mathbf{x}_+^{(j+1)} = \mathbf{x}_-^{(j+1)} + \mathbf{K}^{(j+1)} \mathbf{v}^{(j+1)};$ $\mathbf{P}_+^{(j+1)} = \mathbf{P}_-^{(j+1)} - \mathbf{K}^{(j+1)} \mathbf{S}^{(j+1)} (\mathbf{K}^{(j+1)})^T.$	$\mathbf{Y}_-^{(j+1)} = \mathbf{x}_+^{(j+1)} \mathbf{1}^T + \sqrt{n + \lambda} \begin{bmatrix} 0 & \sqrt{\mathbf{P}_-^{(j+1)}} & -\sqrt{\mathbf{P}_-^{(j+1)}} \end{bmatrix};$ $\hat{\mathbf{Z}}^{(j+1)} = \mathbf{h}(\mathbf{Y}_-^{(j+1)});$ $\mathbf{v}^{(j+1)} = \mathbf{z}^{(j+1)} - \hat{\mathbf{Z}}^{(j+1)} \mathbf{w}_m;$ $\mathbf{S}^{(j+1)} = \hat{\mathbf{Z}}^{(j+1)} \mathbf{W} [\hat{\mathbf{Z}}^{(j+1)}]^T + \mathbf{R}^{(j+1)};$ $\mathbf{C}^{(j+1)} = \mathbf{Y}_-^{(j+1)} \mathbf{W} [\hat{\mathbf{Z}}^{(j+1)}]^T;$ $\mathbf{K}^{(j+1)} = \mathbf{C}^{(j+1)} (\mathbf{S}^{(j+1)})^{-1}.$

Terms used in the **Table 1** have the following meaning:

α, β – smoothing parameters;

$\mathbf{Q} = 10^q \mathbf{I}$ – process noise covariance matrix;

q – parameter of the process noise covariance matrix;

\mathbf{I} – identity matrix;

\mathbf{R} – measurement noise covariance matrix;

\mathbf{a}, \mathbf{b} – $n \times 1$ dimensional level vector and $n \times 1$ dimensional slope vector, respectively, used for determining vector \mathbf{g} ;

$\alpha_{\text{UKF}}, \beta_{\text{UKF}}, \kappa_{\text{UKF}}$ – parameters of unscented transformation;

\mathbf{Y} – $2n+1$ dimensional vector of sigma points;

$w_m^{(0)}, w_c^{(0)}, w_m^{(i)}, w_c^{(i)}$ – weight factors;

λ_{UKF} – scale parameter defined as: $\lambda_{\text{UKF}} = \alpha_{\text{UKF}}^2 (n + \kappa_{\text{UKF}}) - n$;

$\mathbf{x}_-, \mathbf{x}_+$ – predicted state and estimated state vector, respectively;
 $\mathbf{P}_-, \mathbf{P}_+$ – state prediction and state estimation error covariance matrix, respectively;
 \mathbf{F} – state transition matrix;
 $\mathbf{1}$ – vector of all ones;
 \mathbf{g} – vector associated with the trend behavior of the state trajectory;
 $\hat{\mathbf{X}}$ – $n \times (2n+1)$ dimensional matrix made up of sigma points propagated through the process model;
 \mathbf{w}_m – $(2n+1)$ dimensional weight vector defined as:

$$\mathbf{w}_m = \left[\mathbf{w}_m^{(0)} \ \mathbf{w}_m^{(1)} \ \dots \ \mathbf{w}_m^{(2n)} \right];$$

\mathbf{W} – $(2n+1) \times (2n+1)$ dimensional weight matrix defined as:

$$\mathbf{W} = \left(\mathbf{I}_{2n+1} - \mathbf{w}_m \mathbf{1}^T \right) \cdot \text{diag} \left\{ w_c^{(0)} \ w_c^{(1)} \ \dots \ w_c^{(2n)} \right\} \cdot \left(\mathbf{I}_{2n+1} - \mathbf{w}_m \mathbf{1}^T \right);$$

\mathbf{v} – innovation vector;
 \mathbf{S} – innovation covariance matrix;
 \mathbf{H} – Jacobian matrix;
 \mathbf{K} – Kalman gain matrix; and
 \mathbf{C} – cross-covariance matrix of the state and measurement.

3 Modeling of Measurement Noise

WLS, as well as EKF and UKF, usually assume that the measurement noise follows Gaussian distribution. This assumption does not universally hold true in the practical applications. To investigate the impact of non-Gaussian measurement noise on the performance of three state estimators, different non-Gaussian probability density functions have been assigned to measurement noise.

The true measurement vector \mathbf{z}^{true} is obtained via power flow (PF) calculations. The observed (noisy) measurement vector \mathbf{z} is obtained by superimposing the noise to the previously calculated true measurements as [26]:

$$z_i = z_i^{true} \left[1 + \text{RAND}(f) \left(\frac{Acc_i}{300} \right) \right], \quad i = 1, 2, \dots, m, \quad (7)$$

where $\text{RAND}(f)$ is random sample generated from a probability density function f .

We have assumed that measurement noise is independent, identically distributed and subject to one of the following probability distributions [12]: Gaussian and non-Gaussian (Uniform, Laplace, Weibull and Gaussian mixture of two Gaussian components). Considering independency in measurement noise, probability density functions for the analyzed distributions can be expressed via (8) – (12).

– Gaussian:

$$\mathcal{N}(e_i; \mu_i, \sigma_i) = \frac{1}{\sigma_i \sqrt{2\pi}} \exp\left(-\frac{1}{2} \left(\frac{e_i - \mu_i}{\sigma_i}\right)^2\right); \quad -\infty < e_i < \infty, \quad (8)$$

– Uniform:

$$\mathcal{U}(e_i; u_i, v_i) = \frac{1}{(v_i - u_i)}; \quad u_i < e_i < v_i, \quad (9)$$

– Laplace:

$$\mathcal{L}(e_i; \delta_i, d_i) = \frac{1}{2d_i} \exp\left(-\frac{|e_i - \delta_i|}{d_i}\right); \quad -\infty < e_i < \infty, \quad (10)$$

– Weibull:

$$\mathcal{W}(e_i; d_i, c_i) = \frac{c_i}{d_i} \left(\frac{e_i}{d_i}\right)^{c_i-1} \exp\left(-\frac{e_i}{d_i}\right)^{c_i}; \quad e_i \geq 0, \quad (11)$$

– Gaussian mixture of two Gaussian components:

$$\mathcal{N}_{mix}(e_i; w'_i, \mu'_i, \sigma'_i, w''_i, \mu''_i, \sigma''_i) = w'_i \mathcal{N}(e_i; \mu'_i, \sigma'_i) + w''_i \mathcal{N}(e_i; \mu''_i, \sigma''_i); \quad -\infty < e_i < \infty, \quad (12)$$

where:

e_i – noise in i^{th} measurement;

μ_i – mean value;

σ_i – standard deviation;

u_i – lower limit of the range;

v_i – upper limit of the range;

δ_i – location parameter;

d_i – scale parameter;

c_i – shape parameter;

w'_i, w''_i – weights of mixture components;

μ'_i, μ''_i – means of mixture components; and

σ'_i, σ''_i – standard deviations of mixture components.

Random samples, *RAND* (f), were generated for each of the above distributions, where distributions are with the distribution parameters defined in **Table 2**. Distribution parameters are selected as in [12]. Histograms of generated data are shown in Fig. 1 for each of the considered probability distributions.

In Fig. 1, 5000 data samples have been generated in case of each distribution using the program developed in MATLAB. Histograms are graphed in

comparison to the probability density function of standard Gaussian distribution ($\mu_i = 0$, $\sigma_i = 1$). In some cases, as is evident from Fig. 1, distribution of the generated data significantly differs from the commonly assumed Gaussian distribution.

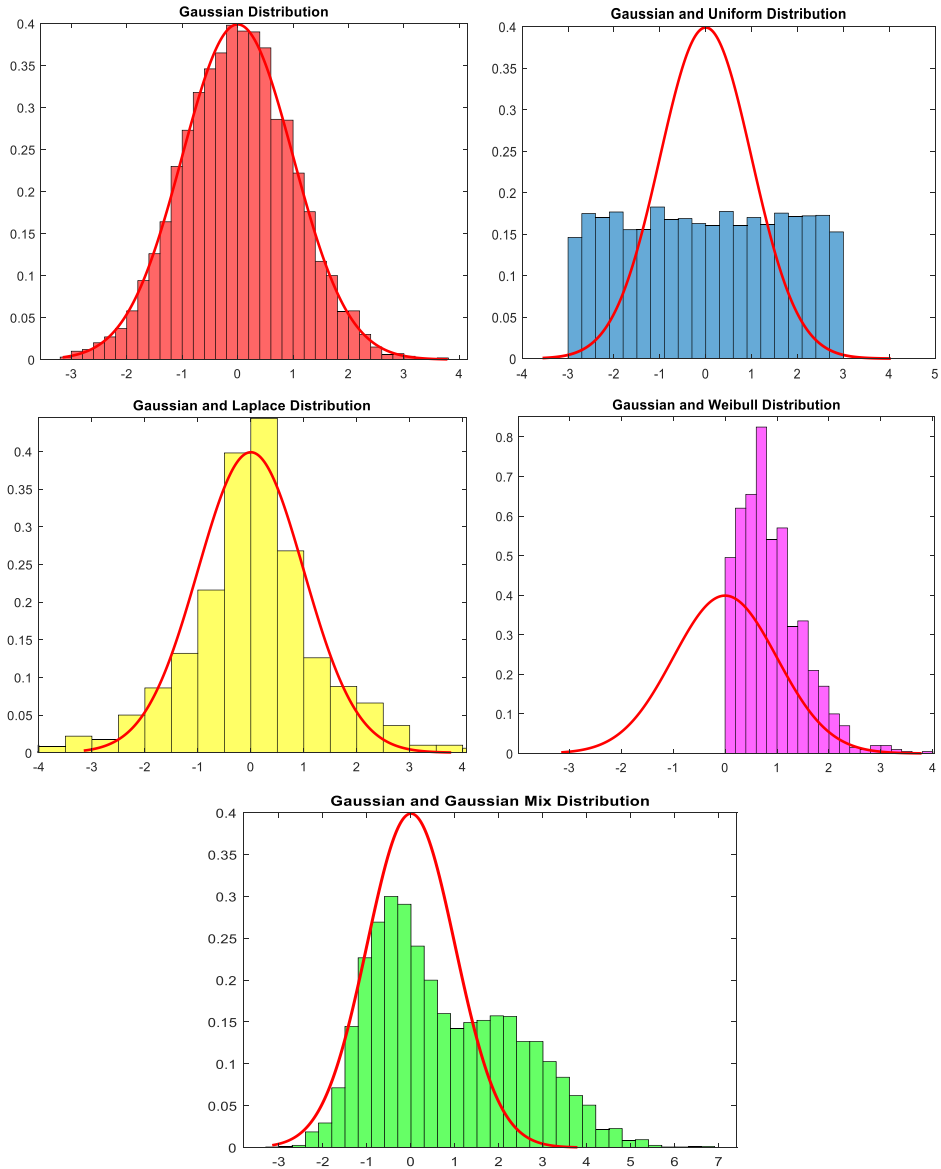


Fig. 1 – Histograms of generated numerical data in comparison with probability density function of standard Gaussian distribution (red curve).

Table 2
Parameter settings for different probability distributions.

Distribution	Distribution parameters
Gaussian	$\mu_i = 0, \sigma_i = 1$
Uniform	$u_i = -3, v_i = 3$
Laplace	$\delta_i = 0, d_i = 1$
Weibull	$d_i = 1, c_i = 1.5$
Gaussian mix	$w'_i = 0.7, w''_i = 0.3, \mu'_i = -0.5, \mu''_i = 2, \sigma'_i = 0.7, \sigma''_i = 1.3$

4 Simulation Results

The influence of the non-Gaussian measurement noise on SE results was tested on modified IEEE 37-bus distribution system, shown in Fig. 2. Test system is modified by connecting photovoltaic (PV) generator of 900 kW rated power at bus 30. Measurement configuration of the modified test system is also depicted in Fig. 2. The observed (noisy) measurements were obtained according to the methodology presented in Section III. Accuracy of the telemetered and pseudo measurements is set as 3% and 50%, respectively. For virtual measurements of zero bus injections a standard deviation of 10^{-5} is adopted.

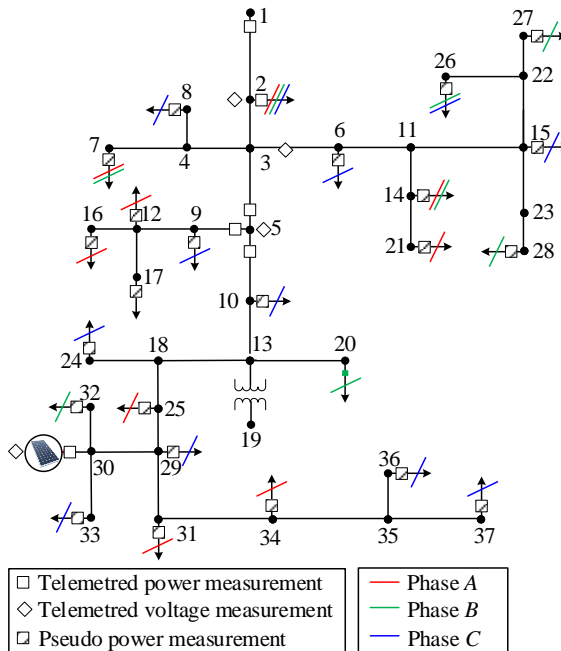


Fig. 2 – Network topology and measurement configuration of modified IEEE 37-bus test system.

State estimation is performed with three different SE methods: WLS, EKF and UKF, described in *Section II*. Execution step of SE is chosen to be 1 min. Simulations were run over a period of one day, giving 1440 sampling points in 24 h. To evaluate and compare the estimation accuracy of SE methods, mean absolute error (MAE) and average mean absolute error (AMAE) calculated over voltage magnitudes and angles are used:

$$\xi_V^{(j),MAE} = \frac{1}{n_V} \sum_{l=1}^{n_V} \left| V_{l+}^{(j)} - V_l^{(j),true} \right|; \quad (13)$$

$$\xi_\theta^{(j),MAE} = \frac{1}{n_\theta} \sum_{l=1}^{n_\theta} \left| \theta_{l+}^{(j)} - \theta_l^{(j),true} \right|; \quad (14)$$

$$\xi_V^{AMAE} = \frac{1}{N} \sum_{j=1}^N \xi_V^{(j),MAE}; \quad (15)$$

$$\xi_\theta^{AMAE} = \frac{1}{N} \sum_{j=1}^N \xi_\theta^{(j),MAE}, \quad (16)$$

where:

n_V – number of elements in vector of voltage magnitudes \mathbf{V} ;

n_θ – number of elements in vector of voltage angles θ .

$V_{l+}^{(j)}$ – estimated value of l^{th} voltage magnitude at j^{th} time sample;

$V_l^{(j),true}$ – true value of l^{th} voltage magnitude at j^{th} time sample;

$\theta_{l+}^{(j)}$ – estimated value of l^{th} voltage angle at j^{th} time sample;

$\theta_l^{(j),true}$ – true value of l^{th} voltage angle at j^{th} time sample; and

N – total number of time samples over simulation period.

The performance of SE methods has been compared under different operating conditions: quasi-steady state, sudden state changes and bad data.

4.1 Quasi-steady state operation

To simulate slow changes in state trajectory, normalized daily load/generation profiles have been assigned to the corresponding buses. Slow changes in the demand and distributed generation, characterized by daily profiles, drive slow changes in the system state. AMAE on voltage magnitudes and angles is shown in the **Table 3** under five different measurement noise distributions.

Comparing the results of WLS, EKF and UKF method that are given in **Table 3**, one can conclude that the EKF method generally shows the best performance in terms of ξ_V^{AMAE} and ξ_θ^{AMAE} for all tested distributions. The Uniform distribution leads to the highest ξ_V^{AMAE} and ξ_θ^{AMAE} (up to

$\xi_{\mathcal{V}}^{AMAE} = 4.79 \times 10^{-4}$ p.u. and $\xi_{\mathcal{S}_0}^{AMAE} = 3.80 \times 10^{-4}$ rad, in case of WLS) causing the poorest estimates among the tested distributions. In contrast to that, Laplace and Weibull distributions lead to lowest estimation errors ($\xi_{\mathcal{V}}^{AMAE} = 1.79 \times 10^{-4}$ p.u. and $\xi_{\mathcal{S}_0}^{AMAE} = 1.04 \times 10^{-4}$ rad, in case of EKF). The mentioned results are highlighted in the **Table 3**.

Table 3

Average Mean Absolute Error (AMAE) on voltage magnitudes and angles in quasi-steady state operation under different measurement noise distributions.

Method Distribution	WLS		EKF		UKF	
	$\xi_{\mathcal{V}}^{AMAE}$ [p.u.]	$\xi_{\mathcal{S}_0}^{AMAE}$ [rad]	$\xi_{\mathcal{V}}^{AMAE}$ [p.u.]	$\xi_{\mathcal{S}_0}^{AMAE}$ [rad]	$\xi_{\mathcal{V}}^{AMAE}$ [p.u.]	$\xi_{\mathcal{S}_0}^{AMAE}$ [rad]
Gaussian	2.74×10^{-4}	2.22×10^{-4}	1.80×10^{-4}	1.50×10^{-4}	2.38×10^{-4}	1.94×10^{-4}
Uniform	4.79×10^{-4}	3.80×10^{-4}	3.15×10^{-4}	2.59×10^{-4}	4.03×10^{-4}	3.29×10^{-4}
Laplace	2.65×10^{-4}	2.21×10^{-4}	1.79×10^{-4}	1.51×10^{-4}	2.38×10^{-4}	1.95×10^{-4}
Weibull	2.91×10^{-4}	1.42×10^{-4}	2.65×10^{-4}	1.04×10^{-4}	2.73×10^{-4}	1.34×10^{-4}
Gaussian mix	4.08×10^{-4}	3.27×10^{-4}	2.77×10^{-4}	2.25×10^{-4}	3.55×10^{-4}	2.86×10^{-4}

Based on the analysis of the results presented in **Table 3**, it is evident that the Laplacian noise impacts the accuracy of estimators similarly as Gaussian noise. As expected, the least resemblance to the results obtained under Gaussian distribution is shown in case when measurement noise follows Uniform distribution. Deviation from the results obtained under Gaussian distribution is also significant in the case of the Gaussian Mixture distribution. Hence, it can be concluded that, during quasi-steady state operation, the accuracy of state estimators is less affected if measurement noise is Laplacian distributed. On the other hand, state estimates will be uncertain the most if measurement noise is distributed according to Uniform or Gaussian Mix distribution.

The process noise covariance matrix is one of the key parameters that impacts the performance of Kalman filter-based state estimators. It models the noise level of the state transition function. This noise level depends on uncertainties in demand and distributed generation, which can vary over the time. Therefore, assessment of the process noise covariance matrix is more difficult task compared to the assessment of the measurement noise covariance matrix. Luckily, most of the time system operates in quasi-steady state which is characterized by almost constant process-noise levels [27]. If matrix \mathbf{Q} is given in parametric form as $\mathbf{Q} = 10^q \mathbf{I}$, this practically means that its parameter q can be set as time-invariant during quasi-steady state operation. Then, parameter q is

assessed based on offline analysis of this operation mode as a value that minimizes the estimation error. The parameter value chosen in this way provides accurate estimates during quasi-steady state operation. In [28], this procedure has been demonstrated considering that measurement noise follows Gaussian distribution. Here, we repeat the same experiment but under various non-Gaussian distributions in order to check whether or not non-Gaussian measurement noise has impact on optimal choice of parameter q . If yes, matrix Q should be readjusted.

In Figs. 3 and 4, ξ_V^{AMAE} and ξ_{θ}^{AMAE} are shown against parameter q in case of EKF and UKF, respectively. Each Kalman filter-based state estimator is tested under different measurement noise distributions. It can be seen that the estimation error sensitivity to changes in parameter q is the same for Gaussian, Uniform, Laplace and Gaussian Mix distribution. The difference is pronounced only in case of Weibull distribution. This difference is noticeable for estimation errors in voltage magnitudes but negligible for estimation errors in voltage angles. When increasing the parameter q above $q = -6$, a rise in estimation error (both ξ_V^{AMAE} and ξ_{θ}^{AMAE}) is generally observed, especially in case of UKF method. When decreasing its value below $q = -6$, there is no big influence on estimation accuracy, in general. It can be concluded that the choice of parameter q will not depend on the type of measurement noise. Therefore, no readjustment of the process noise covariance matrix Q is required in quasi-steady state operation.

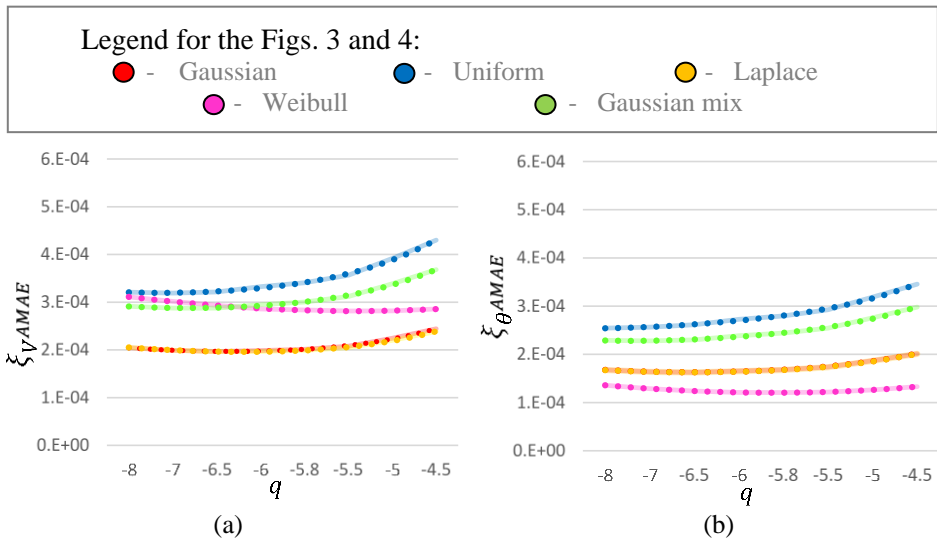


Fig. 3 – Variation of (a) ξ_V^{AMAE} and (b) ξ_{θ}^{AMAE} with respect to parameter q in case of EKF method.

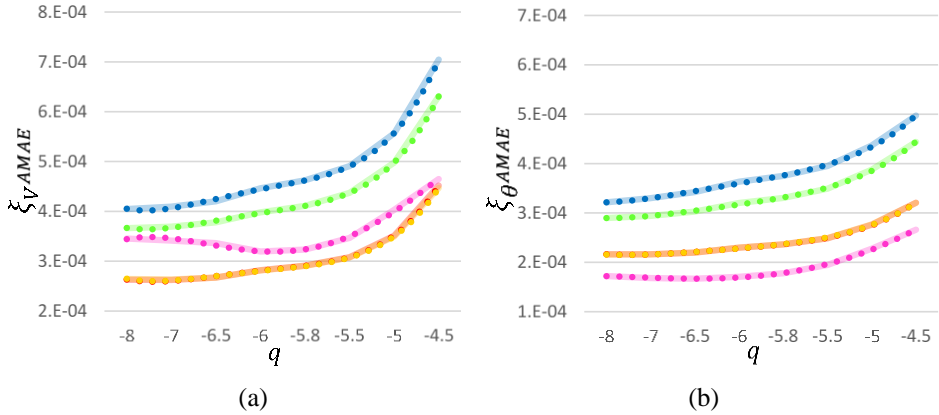


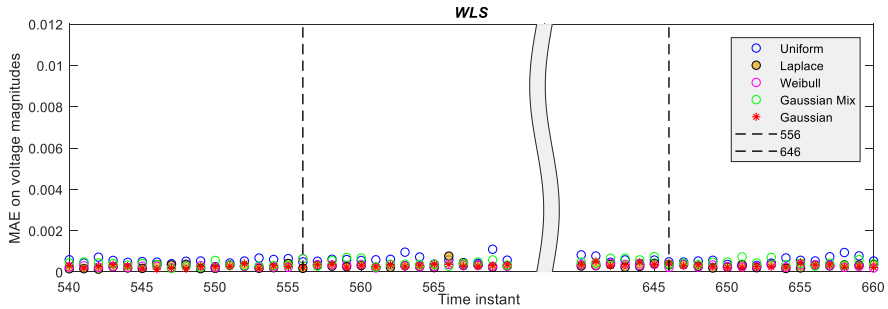
Fig. 4 – Variation of (a) ξ_V^{MAE} and (b) ξ_{θ}^{MAE} with respect to parameter q in case of UKF method.

4.2 Sudden state changes

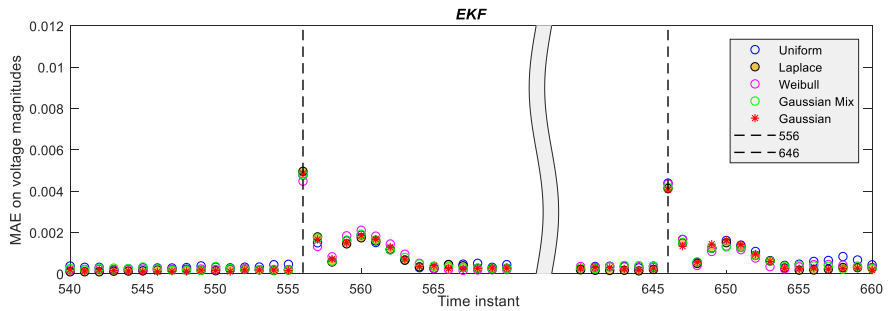
For an additional analysis of the impact of non-Gaussian measurement noise on the performance of the distribution system SE, an abrupt change in the system state, caused by sudden generation change, is considered. In this paper, sudden generation change is simulated twice at node 30. At $j=556$, PV generator is disconnected from the network. Just before disconnection, PV generator operated at its rated power. At $j=646$, PV generator is reconnected to the network. After reconnection, PV generator operated at 85% of its rated power due to less solar irradiance. The MAE is calculated on voltage magnitudes and angles at each time instant j during the simulation period, in the existence of both Gaussian and non-Gaussian measurement noise. The results are shown in Figs.5 and 6 for the time samples before and after the moment of the sudden generation change (denoted by a dashed line).

As can be seen from Figs. 5 and 6, when abrupt change in power generation happens, the MAEs in voltage magnitudes and angles ($\xi_V^{(556),MAE}$ and $\xi_{\theta}^{(646),MAE}$) obtained by Kalman filter based estimators increase sharply regardless of the type of measurement noise. This is because process noise covariance matrix \mathbf{Q} is not adapted to the ongoing changes in the system state but kept constant and equal to optimal matrix for quasi-steady state operation. Comparing the results at time instants $j=556$ and $j=646$, it can be seen that MAE of the Kalman filter based estimators is higher if change in the injected power is higher (MAE at $j=556$ is higher than MAE at $j=646$). However, impact on estimation accuracy is the same in case of Gaussian and non-Gaussian measurement noise. Therefore, the actions required to reduce the estimation error in case of Gaussian noise should be also taken if measurement noise is non-Gaussian distributed. WLS is insensitive to

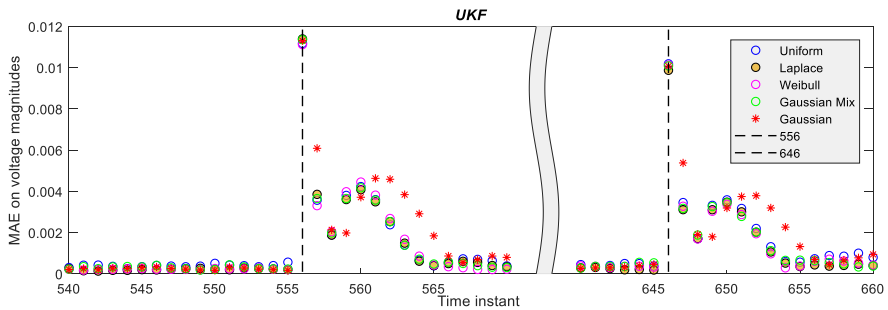
sudden state changes since it utilizes the current snapshot of measurements only and, therefore, is not affected by the abrupt changes in the state trajectory. At the moment of sudden generation change, WLS maintains the same estimation accuracy as in quasi-steady state operation regardless of the type of measurement noise. It can be deduced that the state estimator's performance under sudden state change remains unaffected by the type of the measurement noise.



(a)



(b)



(c)

Fig. 5 – The mean absolute error (MAE) on voltage magnitudes obtained by (a) WLS, (b) EKF and (c) UKF in the presence of Gaussian and non-Gaussian noise.

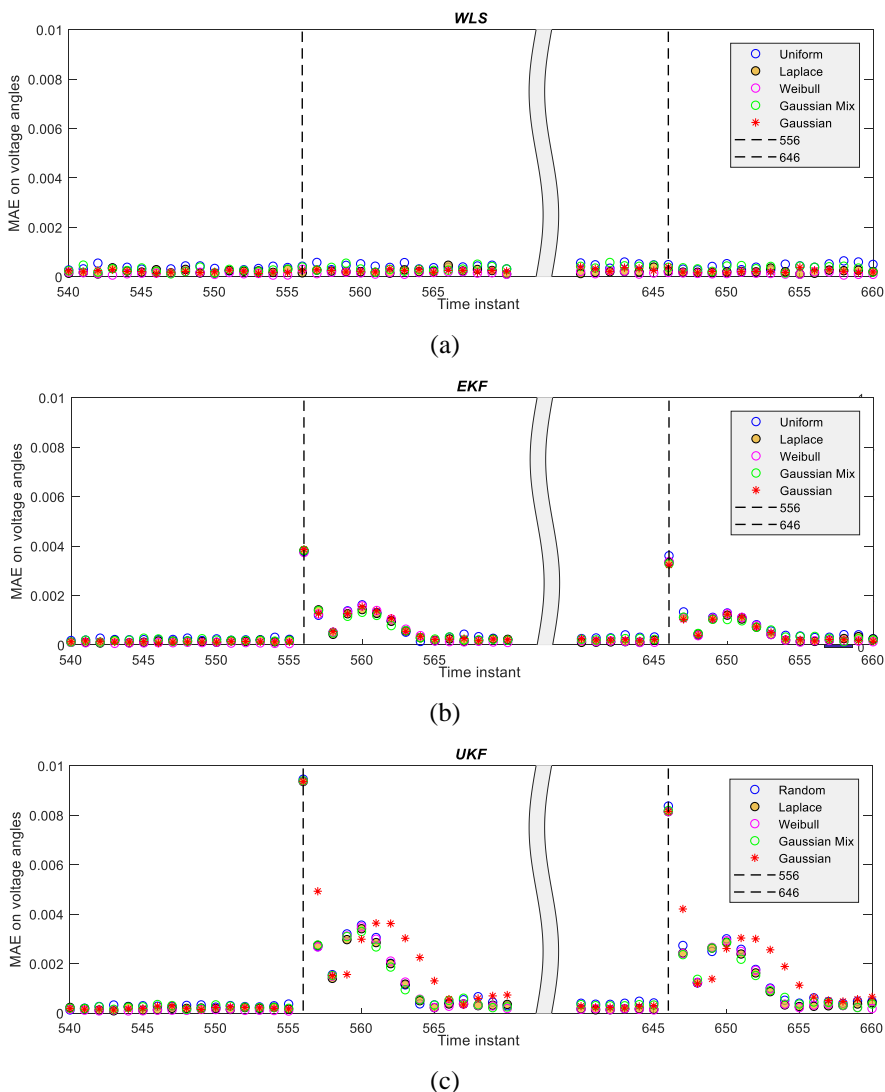


Fig. 6 – The mean absolute error (MAE) on voltage angles obtained by (a) WLS, (b) EKF and (c) UKF in the presence of Gaussian and non-Gaussian noise.

4.3 Bad data

To analyze the impact of measurement noise on state estimators performance with integrated bad data detectors, the following case study has been conducted. WLS estimator has been extended with Largest Normalized Residual (LNR) test to enable bad data detection. LNR test is based on determination of the measurement with the largest value of normalized residual, and comparison of

that value with the prespecified threshold. If largest normalized residual is higher than prespecified threshold, measurement is suspected as bad; otherwise, there is no bad data in the measurement set. Note that performing the LNR test only makes sense if it is done on telemetered measurements. Accordingly, steps in LNR test are [15]:

1. Calculate normalized measurement residuals associated with telemetered measurements:

$$r_i^{(j),nor} = \frac{|z_i^{(j)} - h_i(\mathbf{x}_+^{(j)})|}{\sqrt{\Omega_{ii}^{(j)}}}, \quad i=1,2,\dots,m_{tel}, \quad (17)$$

where $\Omega_{ii}^{(j)}$ is i^{th} diagonal element of residual covariance matrix $\Omega^{(j)} = \mathbf{R}^{(j)} - \mathbf{H}^{(j)}[\mathbf{G}^{(j)}]^{-1}[\mathbf{H}^{(j)}]^T$ at time j , and the count of telemetered measurements in the measurement set is represented by m_{tel} .

2. Find the largest measurement residual: $LNR^{(j)} = \max_i \{r_i^{(j),nor}\}$;
3. Compare $LNR^{(j)}$ with t , where t is the detection threshold;
4. If $LNR^{(j)} > t$, measurement is suspected as bad data; otherwise, in the j^{th} snapshot, there is no suspected measurement.

Considering statistical properties of the Gaussian noise, threshold t in LNR test is usually set to $t = 3$ [15, 29]. False positive is the case in which LNR test indicates bad data presence although there is no bad data in the measurement set. To further reduce the number of false positives in case of Gaussian measurement noise, this threshold can be set higher than $t = 3$. Conversely, the threshold should not be placed at an overly high value; otherwise, LNR test may fail to recognize bad data of small intensity. Therefore, in this paper, we set it to $t = 3.5$. Using this setting, the performance of WLS estimator with integrated LNR test is analyzed for both Gaussian and non-Gaussian measurement noise. In Fig. 7, LNR obtained under Gaussian and non-Gaussian measurement noise in the absence of bad data is displayed for the entire simulation period.

While LNR obtained in the presence of Gaussian measurement noise remains below the threshold almost all the time, in case of non-Gaussian measurement noise LNR very often transcends the threshold, resulting in a huge number of false positives. This is because non-Gaussian measurement noise can have a long and/or thick tails. Characteristics of these tails depend on the type and the distribution parameters of the specific non-Gaussian probability density function. Table 3 summarizes the numbers of false positives in case of different types of measurement noise. While the prespecified detection threshold can be considered as suitable for the Gaussian measurement noise, the rate of false positives is

unacceptably high in case of non-Gaussian measurement noise. This is especially true for Uniform and Gaussian Mixture distribution, where bad data is wrongly detected at every sixth time instant on average.

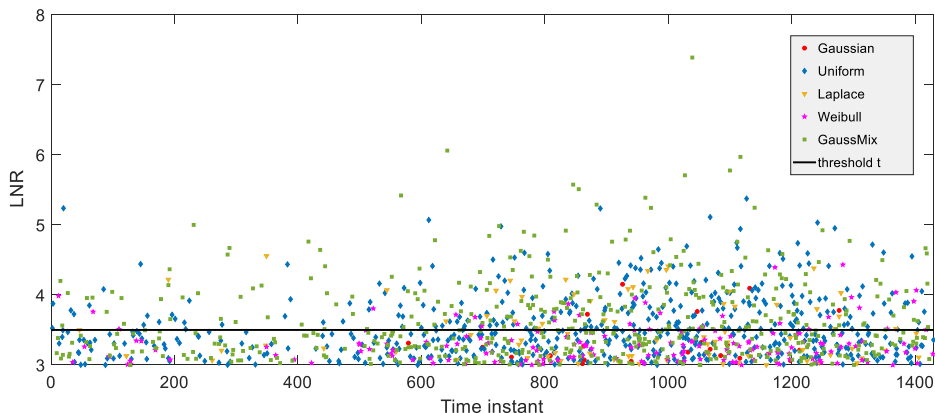


Fig. 7 – *LNR without the presence of bad data while taking into account various distributions of the measurement noise.*

Obviously, non-Gaussian measurement noise can affect the performance of the traditional bad data detector. Therefore, if measurement noise is not Gaussian distributed, new detection threshold adjusted to the properties of the specific non-Gaussian probability density function has to be selected.

Table 3

False positives of LNR test depending on the probability density function of the measurement noise.

Probability density function of the measurement noise	No. of false positives	False positives rate [%]
Gaussian	5	0.3
Uniform	238	16.5
Laplace	31	2.1
Weibull	33	2.3
Gaussian Mixture	224	15.5

5 Conclusion

In this paper, impact of non-Gaussian measurement noise on distribution system state estimation is studied, where three different state-of-the-art estimation methods - WLS, EKF and UKF are considered. Impact has been analyzed in terms of estimation accuracy, optimal setting of the process noise covariance matrix and performance of traditional bad data detector. Investigation

has been done utilizing Uniform, Laplace, Weibull and Gaussian mixture as representatives of non-Gaussian probability distributions. As a benchmark, results obtained under Gaussian measurement noise are used. In quasi-steady state operation, non-Gaussian measurement noise can introduce more uncertainty into state estimates, depending on the specific type of non-Gaussian distribution. In case of Kalman filter-based estimation methods, non-Gaussian measurement noise generally does not impact the optimal choice of the process noise covariance matrix for quasi-steady state. Performance of all three state estimators in case of sudden state changes remains unaffected by non-Gaussian measurement noise. However, non-Gaussian noise can significantly affect the performance of traditional bad data detectors, such as Largest Normalized Residual test, requiring readjustment of the detection threshold. As one of the future research directions, investigation can be extended considering that non-Gaussian noise is not independent and identically distributed.

6 Acknowledgment

This study was supported by the Ministry of Science, Technological Development and Innovation of the Republic of Serbia, and these results are part of the Grant No. 451-03-66 / 2024-03 / 200132 with University of Kragujevac – Faculty of Technical Sciences Čačak.

7 References

- [1] H. Liu, J. Li, J. Li, J. Tian, T. Bi, K. E. Martin, Q. Yang: Synchronised Measurement Devices for Power Systems with High Penetration of Inverter-Based Renewable Power Generators, *IET Renewable Power Generation*, Vol. 13, No. 1, January 2019, pp. 40–48.
- [2] X. Ji, Z. Yin, Y. Zhang, M. Wang, X. Zhang, C. Zhang, D. Wang: Real-Time Robust Forecasting-Aided State Estimation of Power System Based on Data-Driven Models, *International Journal of Electrical Power & Energy Systems*, Vol. 125, February 2021, p. 106412.
- [3] H. Dehra: Characterization of Noise in Power Systems, *Proceedings of the International Conference on Power Energy, Environment and Intelligent Control (PEEIC)*, Greater Noida, India, April 2018, pp. 320–329.
- [4] M. Brown, M. Biswal, S. Brahma, S. J. Ranade, H. Cao: Characterizing and Quantifying Noise in PMU Data, *Proceedings of the IEEE Power and Energy Society General Meeting (PESGM)*, Boston, USA, July 2016, pp. 1–5.
- [5] J. Liu, J. Tang, F. Ponci, A. Monti, C. Muscas, P. A. Pegoraro: Trade-offs in PMU Deployment for State Estimation in Active Distribution Grids, *IEEE Transactions on Smart Grid*, Vol. 3, No. 2, June 2012, pp. 915–924.
- [6] P. A. Pegoraro, J. Tang, J. Liu, F. Ponci, A. Monti, C. Muscas: PMU and Smart Metering Deployment for State Estimation in Active Distribution Grids, *Proceedings of the IEEE International Energy Conference and Exhibition (ENERGYCON)*, Florence, Italy, September 2012, pp. 873–878.

- [7] M. Pau, P. A. Pegoraro, S. Sulis: WLS Distribution System State Estimator Based on Voltages or Branch-Currents: Accuracy and Performance Comparison, Proceedings of the IEEE International Instrumentation and Measurement Technology Conference (I2MTC), Minneapolis, USA, May 2013, pp. 493–498.
- [8] A. Angioni, M. Pau, F. Ponci, A. Monti, C. Muscas, S. Sulis, P. A. Pegoraro: Bayesian Distribution System State Estimation in Presence of Non-Gaussian Pseudo-Measurements, Proceedings of the IEEE International Workshop on Applied Measurements for Power Systems (AMPS), Aachen, Germany, September 2016, pp. 1–6.
- [9] P. A. Pegoraro, A. Angioni, M. Pau, A. Monti, C. Muscas, F. Ponci, S. Sulis: Bayesian Approach for Distribution System State Estimation with Non-Gaussian Uncertainty Models, IEEE Transactions on Instrumentation and Measurement, Vol. 66, No. 11, November 2017, pp. 2957–2966.
- [10] R. Mínguez, A. J. Conejo, A. S. Hadi: Non Gaussian State Estimation in Power Systems, Advances in Mathematical and Statistical Modeling – Statistics for Industry and Technology, Birkhäuser, Boston, 2008.
- [11] Q. Shi, M. Liu, L. Hang: A Novel Distribution System State Estimator Based on Robust Cubature Particle Filter Used for Non-Gaussian Noise and Bad Data Scenarios, IET Generation, Transmission & Distribution, Vol. 16, No. 7, April 2022, pp. 1385–1399.
- [12] R. Martínez-Parrales, C. R. Fuerte-Esquivel, B. A. Alcaide-Moreno: Analysis of Bad Data in Power System State Estimation Under Non-Gaussian Measurement Noise, Electric Power Systems Research, Vol. 186, September 2020, p. 106424.
- [13] A. Tollkühn, F. Particke, J. Thielecke: Gaussian State Estimation with Non-Gaussian Measurement Noise, Proceedings of the Sensor Data Fusion: Trends, Solutions, Applications (SDF), Bonn, Germany, October 2018, pp. 1–5.
- [14] G. Valverde, V. Terzija: Unscented Kalman filter for Power System Dynamic State Estimation, IET Generation, Transmission & Distribution, Vol. 5, No. 1, January 2011, pp. 29–37.
- [15] A. Abur, A. G. Exposito: Power System State Estimation – Theory and Implementation, Marcel Dekker, Inc., New York, Basel, 2004.
- [16] F. C. Schweppe, J. Wildes: Power System Static-State Estimation, Part I: Exact Model, IEEE Transactions on Power Apparatus and Systems, Vol. Pas-89, No. 1, January 1970, pp. 120–125.
- [17] R. Singh, B. C. Pal, R. A. Jabr: Distribution System State Estimation Through Gaussian Mixture Model of the Load as Pseudo-Measurement, IET Generation, Transmission & Distribution, Vol. 4, No. 1, January 2010, pp. 50–59.
- [18] A. Monticelli: State Estimation in Electric Power Systems: A Generalized Approach, Springer, New York, 1999.
- [19] F. C. Aschmoneit, N. M. Peterson, E. C. Adrian: State Estimation with Equality Constraints, Proceedings of the 10th IEEE Power Industry Computer Applications Conference (PICA), Toronto, Canada, May 1977, pp. 427–430.
- [20] G. N. Korres: A Robust Method for Equality Constrained State Estimation, IEEE Transactions on Power Systems, Vol. 17, No. 2, May 2002, pp. 305–314.
- [21] A. M. Leite da Silva, M. B. Do Coutto Filho, J. F. de Queiroz: State Forecasting in Electric Power Systems, IEE Proceedings C (Generation, Transmission and Distribution), Vol. 130, No. 5, September 1983, pp. 237–244.
- [22] F. Gustafsson, G. Hendeby: Some Relations Between Extended and Unscented Kalman Filters, IEEE Transactions on Signal Processing, Vol. 60, No. 2, February 2012, pp. 545–555.

- [23] E. A. Wan, R. Van Der Merwe: The Unscented Kalman Filter for Nonlinear Estimation, Proceedings of the IEEE Adaptive Systems for Signal Processing, Communications, and Control Symposium, Lake Louise, Canada, October 2000, pp. 153-158.
- [24] S. J. Julier, J. K. Uhlmann: Unscented Filtering and Nonlinear Estimation, Proceedings of the IEEE, Vol. 92, No. 3, March 2004, pp. 401 – 422.
- [25] S. Särkkä: Recursive Bayesian Inference on Stochastic Differential Equations, PhD Dissertation, Helsinki University of Technology, Helsinki, Finland, 2006.
- [26] D. H. Tungadio, J. A. Jordaan, M. W. Siti: Power System State Estimation Solution Using Modified Models of PSO Algorithm: Comparative Study, Measurement, Vol. 92, October 2016, pp. 508 – 523.
- [27] A. M. Leite da Silva, M. B. Do Coutto Filho, J. M. C. Cantera: An Efficient Dynamic State Estimation Algorithm Including Bad Data Processing, IEEE Transactions on Power Systems, Vol. 2, No. 4, November 1987, pp. 1050 – 1058.
- [28] D. N. Četenović, A. M. Ranković: Optimal Parameterization of Kalman Filter Based Three-Phase Dynamic State Estimator for Active Distribution Networks, International Journal of Electrical Power & Energy Systems, Vol. 101, October 2018, pp. 472 – 481.
- [29] N. Veerakumar, D. Četenović, K. Kongurai, M. Popov, A. Jongepier, V. Terzija: PMU-Based Real-Time Distribution System State Estimation Considering Anomaly Detection, Discrimination and Identification, International Journal of Electrical Power & Energy Systems, Vol. 148, June 2023, p. 108916.